Electronic Supplementary Material (ESI) for Physical Chemistry Chemical Physics.

Supporting Information

A first peek into sub-picosecond dynamics of spin energy levels in magnetic biomolecules

Lorena E. Rosaleny,[1,2] Kirill Zinovjev,[1] Iñaki Tuñón,[1] Alejandro Gaita-Ariño[2]
[1] Departament de Química Física, Universitat de València, 46100 Burjassot, Spain
[2] Instituto de Ciencia Molecular, Universitat de València, 46980 Paterna, Spain

List of contents

S1. System preparation

We extracted one calcium bound LBT molecule (see Fig. 1a from manuscript) from the Protein Data Bank (ID code 1TJB),[1] and stripped all the waters and ions not necessary for the structural integrity. Subsequently input files required for the terbium were created using MD parameters for the Tb^{3+} ion obtained from Quiao et al.[2], and this new PDB file was used to create a system consisting of a molecule of TbLBT situated in the middle of a cubic box (side 41.9 Å) of (20% glycerol in water) solvent using the Packmol program.[3] Two Na^+ ions were added to ensure the neutrality of the system. The five negative charges in the LBT peptide are countered by the three positive charges belonging to terbium, and the two positive charges contributed by the Na^+ ions. The cubic box generated was comprised also by 1884 water molecules and 116 glycerol molecules (Fig. S1). This ensured that the MD simulations were performed in a mixture of water/glycerol mimicking experimental samples for previous EPR experiments.[4]

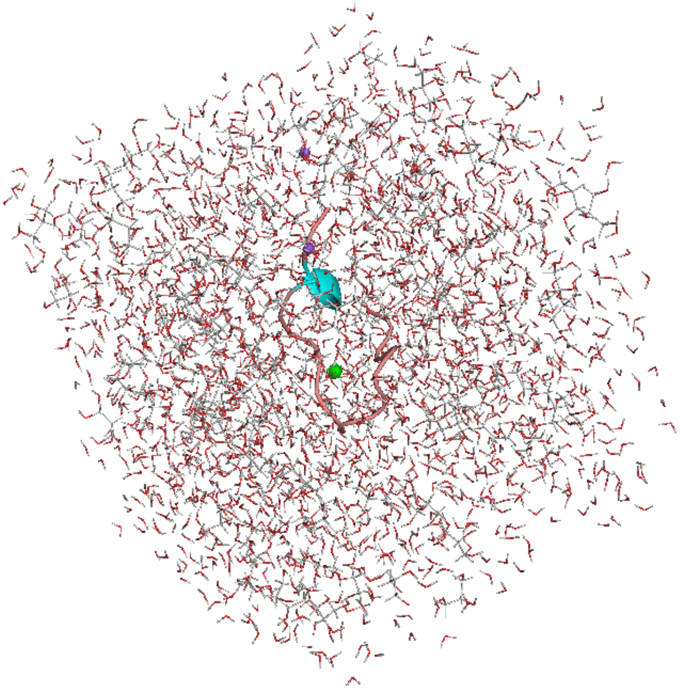

Figure S1. *Visualization of the final PDB file created with the packmol software corresponding to the TbLBT molecule in a solvent box. The cubic box contains LBT (cartoon format), a* Tb^{3+} *ion (green sphere),* Na^+ *ions (purple spheres), and a mixture water-glycerol (stick format) as solvent. The image was generated via PyMOL version 1.7.2.1.*

S2. Validation of the Force Field using B3LYP

The quality of the MM potential employed to describe Terbium-protein interactions has been tested comparing the structural model obtained from our simulations with the result of a cluster calculation at B3LYP level, using the CEP-31G basis set. The cluster included the metal and the surrounding residues with a total of 102 atoms. Starting from a structure selected from the 3 K MD simulation we optimized the complex at the QM level. The resulting structure (see Fig. S2) is very similar to the initial one, keeping the same coordination and thus validating the MM force field employed in our work. The distances of the metal to the closest protein oxygen atom are very similar in the QM and MM descriptions (2.26 and 2.27 Å, respectively). The distances to the rest of oxygen atoms forming the first coordination shell are longer at the QM level than in the MM treatment (typically by 0.1-0.2 Å). In spite of this difference, the overall picture obtained at the two theoretical levels for Tb^{3+} coordination are remarkably similar.

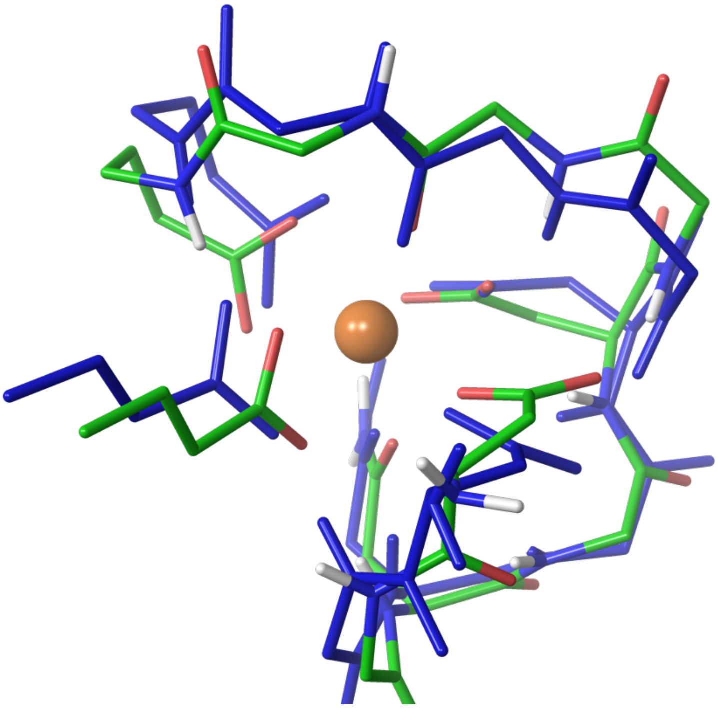

Figure S2. *Cluster model of Terbium coordination by TbLBT. The structure colored in green/blue/red/white is obtained with the MM potential used in MD simulations while the structure colored in blue is obtained after B3LYP/CEP-31G optimization. Nonpolar hydrogen atoms are not represented for clarity.*

***Table S2**. Coordinates of the Tb^{3+} complex optimized at the B3LYP/cep-31G level represented in Figure S2.*

Center	Atomic	Atomic	Coordinates (Angstroms)		
Number	Number	Type	X	Y	Z
1	7	0	-0.097992	-2.713197	4.762617
2	1	0	0.615677	-3.253891	5.257676
3	6	0	0.355716	-2.270604	3.421243
4	1	0	-0.516088	-2.055413	2.787463
5	6	0	1.261034	-0.984875	3.467514
6	1	0	0.694170	-0.193162	3.993071
7	1	0	2.184893	-1.184506	4.031616
8	6	0	1.633815	-0.430501	2.074416
9	8	0	2.806462	0.075556	1.871980
10	8	0	0.710143	-0.497598	1.144948
11	6	0	1.172138	-3.438021	2.812507
12	8	0	2.031785	-4.060867	3.520833
13	7	0	0.930564	-3.729192	1.484067
14	1	0	0.162734	-3.255545	0.978080
15	6	0	1.680235	-4.795109	0.804856
16	1	0	2.291690	-5.317802	1.553500
17	6	0	2.636291	-4.348834	-0.330626
18	8	0	3.381101	-5.218575	-0.887956
19	7	0	2.611214	-3.019639	-0.728173
20	1	0	1.889276	-2.390024	-0.370550
21	6	0	3.374912	-2.604829	-1.921807
22	1	0	4.010561	-3.465140	-2.182056
23	6	0	2.450622	-2.324382	-3.157452
24	1	0	3.078804	-2.221391	-4.053784
25	1	0	1.775649	-3.186673	-3.289193
26	6	0	1.597331	-1.064884	-2.954476
27	8	0	1.016295	-0.874385	-1.818647
28	7	0	1.498852	-0.164624	-3.959062
29	1	0	0.994629	0.725733	-3.771161
30	1	0	2.028630	-0.286109	-4.816881
31	6	0	4.355427	-1.410958	-1.728740
32	8	0	5.063940	-1.051955	-2.727672
33	7	0	4.439599	-0.805844	-0.496974
34	1	0	3.818660	-1.066180	0.271508

35	6	0	5.459128	0.224768	-0.225578
36	1	0	5.790290	0.121767	0.819838
37	6	0	5.040612	1.707606	-0.420687
38	8	0	5.947024	2.597332	-0.501585
39	7	0	3.690715	1.997317	-0.440972
40	1	0	3.017871	1.241776	-0.300760
41	6	0	3.208352	3.390714	-0.515097
42	1	0	4.093032	4.009435	-0.728909
43	6	0	2.179903	3.617042	-1.669118
44	1	0	1.723917	4.611367	-1.528109
45	1	0	2.701701	3.616186	-2.637869
46	6	0	1.057793	2.556972	-1.768343
47	8	0	0.644616	2.209428	-2.933976
48	8	0	0.583592	2.030954	-0.639610
49	6	0	2.639462	3.938255	0.823438
50	8	0	2.311691	5.167649	0.905133
51	7	0	2.478258	3.057615	1.870195
52	1	0	2.743473	2.070066	1.774687
53	6	0	1.839995	3.502418	3.116791
54	1	0	2.092428	2.802661	3.927059
55	1	0	2.208257	4.502504	3.391110
56	6	0	0.290395	3.623806	3.059408
57	8	0	-0.353484	3.990495	4.097834
58	7	0	-0.316415	3.341306	1.856401
59	1	0	0.220885	2.984377	1.055073
60	6	0	-1.760125	3.495770	1.687493
61	1	0	-2.151291	4.075619	2.537045
62	6	0	-2.480763	2.128880	1.592880
63	8	0	-1.832011	1.068298	1.294184
64	7	0	-3.827322	2.120734	1.804078
65	1	0	-4.307515	3.003048	1.979953
66	6	0	-4.683643	0.944104	1.508244
67	1	0	-4.038652	0.064251	1.411475
68	6	0	-5.483953	1.221133	0.205750
69	8	0	-6.266703	2.230795	0.148321
70	7	0	-5.274276	0.338122	-0.819559
71	1	0	-4.532637	-0.370088	-0.707083
72	6	0	-5.835992	0.597332	-2.167452
73	1	0	-6.850408	1.002874	-2.030067
74	6	0	-5.005179	1.620248	-3.010116
75	1	0	-5.643777	1.949819	-3.852927

```
     76          1           0       -4.800159    2.504521   -2.387745
     77          6           0       -3.673692    1.068840   -3.598290
     78          1           0       -3.832835    0.138577   -4.169744
     79          1           0       -3.254617    1.812267   -4.302725
     80          6           0       -2.578900    0.793033   -2.557957
     81          8           0       -1.721071   -0.186135   -2.749444
     82          8           0       -2.481274    1.513747   -1.467137
     83          6           0       -5.244756   -5.031966    0.909475
     84          1           0       -4.620050   -5.835889    1.340365
     85          6           0       -4.469032   -3.684946    0.863253
     86          1           0       -5.112480   -2.888133    0.451838
     87          1           0       -4.195653   -3.377640    1.889628
     88          6           0       -3.177672   -3.794023   -0.000117
     89          1           0       -2.491107   -4.554164    0.407573
     90          1           0       -3.446560   -4.111595   -1.026605
     91          6           0       -2.407280   -2.471238   -0.123303
     92          8           0       -1.094240   -2.465917   -0.077919
     93          8           0       -3.032142   -1.337674   -0.288948
     94         65           0       -0.729160    0.029201   -0.522230
     95          1           0       -6.157475   -4.945323    1.525558
     96          1           0       -5.549104   -5.348352   -0.105948
     97          1           0        0.988862   -5.529872    0.356411
     98          1           0       -5.911513   -0.369246   -2.695909
     99          1           0        6.317245    0.063155   -0.891208
    100          1           0       -5.397176    0.804953    2.336251
    101          1           0       -1.972984    4.035672    0.748066
    102          1           0       -0.517051   -1.974433    5.329646
 ---------------------------------------------------------------------
```

S3. MD protocol

An overview of the different steps involved in the molecular dynamics calculations during this work is represented in the scheme below (Fig. S3). The NPT ensemble and pmemd program from the Amber2017 package were employed,[5] together with the ff14SB force field for the peptide[6] and the TIP3P pairwise additive model for water.[7] Glycerol molecules were parameterized using Antechamber.[8] The MD setup was identical for simulations at the three temperatures studied (300 K, 30 K and 3 K). The temperature and pressure were controlled using Langevin thermostat and Berendsen barostat respectively. The timestep in all cases was 2 fs with bonds involving hydrogens fixed using SHAKE.[9]

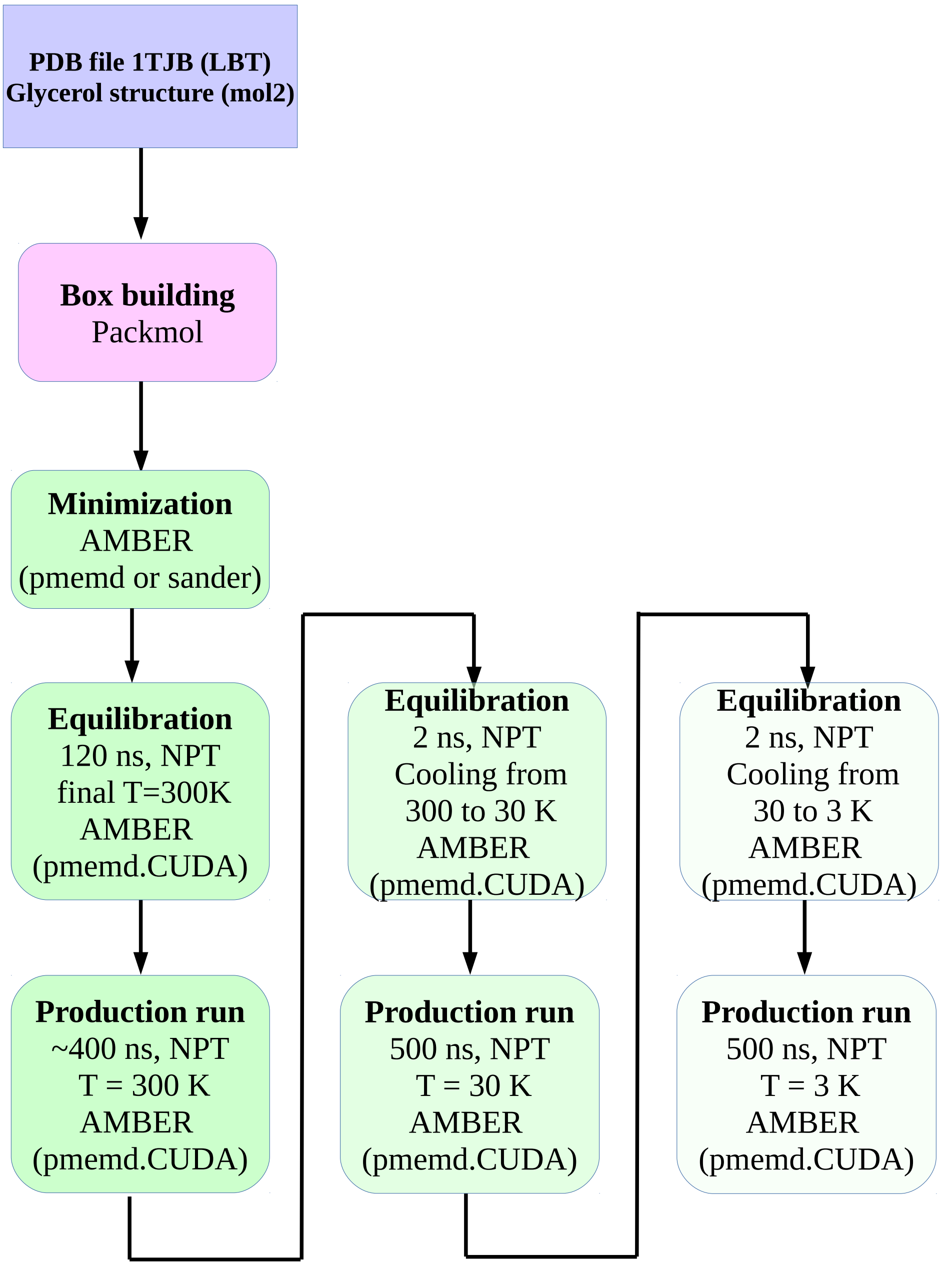

Figure S3. *Workflow showing the MD stages that this work entailed. Three different production runs were performed at three different temperatures (300K, 30 K and 3K).*

Before the actual molecular dynamics simulation was perfomed a minimization in two stages was carried out. The first stage only minimized the solvent (water and glycerol molecules) in the box, and kept the peptide and ions in a fixed position (using cartesian restraints). This stage consisted in a total of 1000 cycles, the first 500 cycles using the steepest descent method, and the final 500 cycles using the conjugate gradient minimization. The second stage of the minimization included all the components of the system (TbLBT, Na^+ ions, water and glycerol), and was performed during 2000 cycles. The first 500 cycles employed the steepest descent algorithm, and the last 1500 cycles used the conjugate gradient method.

The simulation protocol was as follows: first, the system was heated during 1 ns from 0 K to 300 K, and then was equilibrated at 300 K for 120 ns in the NPT ensemble at a pressure of 1 bar. The production run for this temperature had a duration of 390 ns. The last frame of the simulation at 300 K was used for the production run at 30 K by gradually lowering the temperature from 300 to 30 K during 1 ns and then equilibrating the system during the next ns at 30 K. The same protocol was used to initiate the production simulation at 3 K. For 30 K and 3 K the production simulation had a duration of 500 ns.

S4. Quantification of quantum effects employing RPMD

Zero-point energies (ZPE), which are not considered in a classical treatment, can increase the magnitude of structural fluctuations. However, this effect can be compensated, at least partially, by differences in the probability distribution between quantum and classical oscillators. In the quantum picture the probability maxima is found for zero displacement, while in the classical picture the maxima are found at the extreme positions. These two effects go in opposite directions regarding the influence of vibrational fluctuations on the spin energy levels. To further investigate the possible impact of quantum effects on our results obtained at the lowest temperature, we have run a 100 ps long ring polymer molecular dynamics (RPMD) simulation, which allows to include statistical description of nuclear quantum effects in classical MD simulations.[10]

The RPMD calculations were performed using I-PI force engine.[11] Each atom was described by a 32-bead ring polymer. Forces were provided through sander Fortran API using the same potential as for the classical simulations. The system was thermostated at 3 K using path integral Langevin equation.[12]

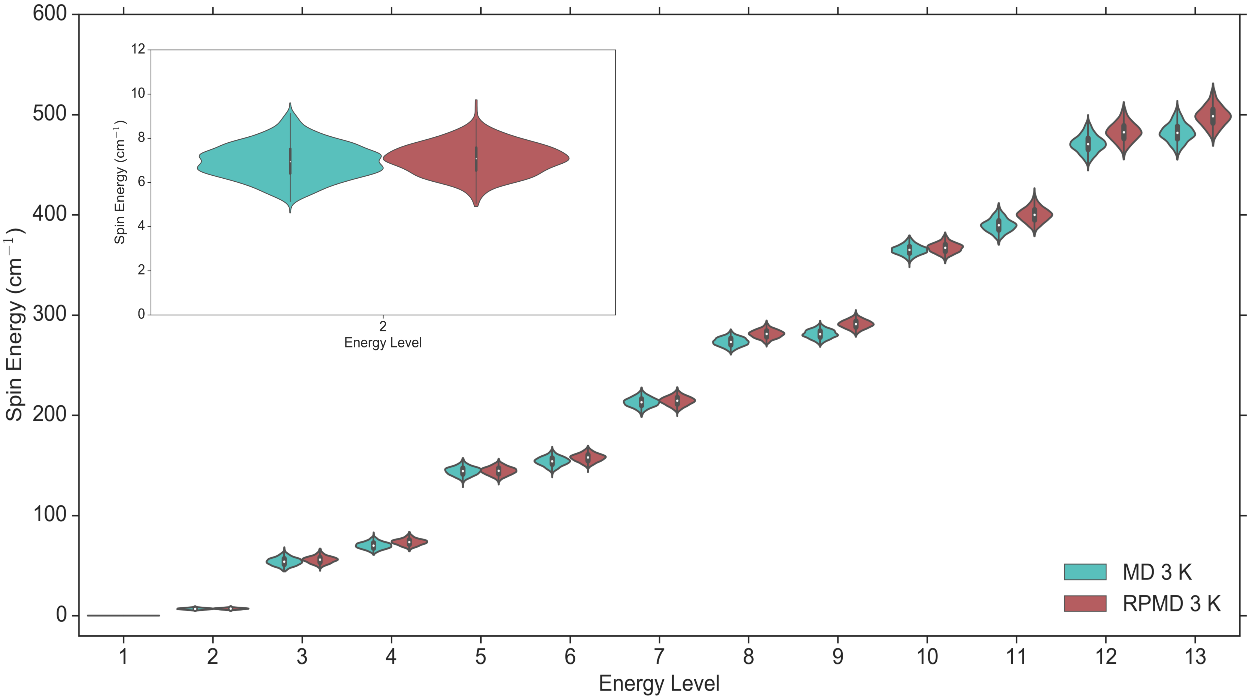

Figure S4.1. *Comparison between the violin plots of the spin energy level distributions over a 1000 MD timesteps (a total of 100 ps) in the ground J multiplet of TbLBT at 3 K calculated by either AMBER MD, the technique employed in this work, or Ring Polymer Molecular Dynamics, which accounts for nuclear quantum effects.*

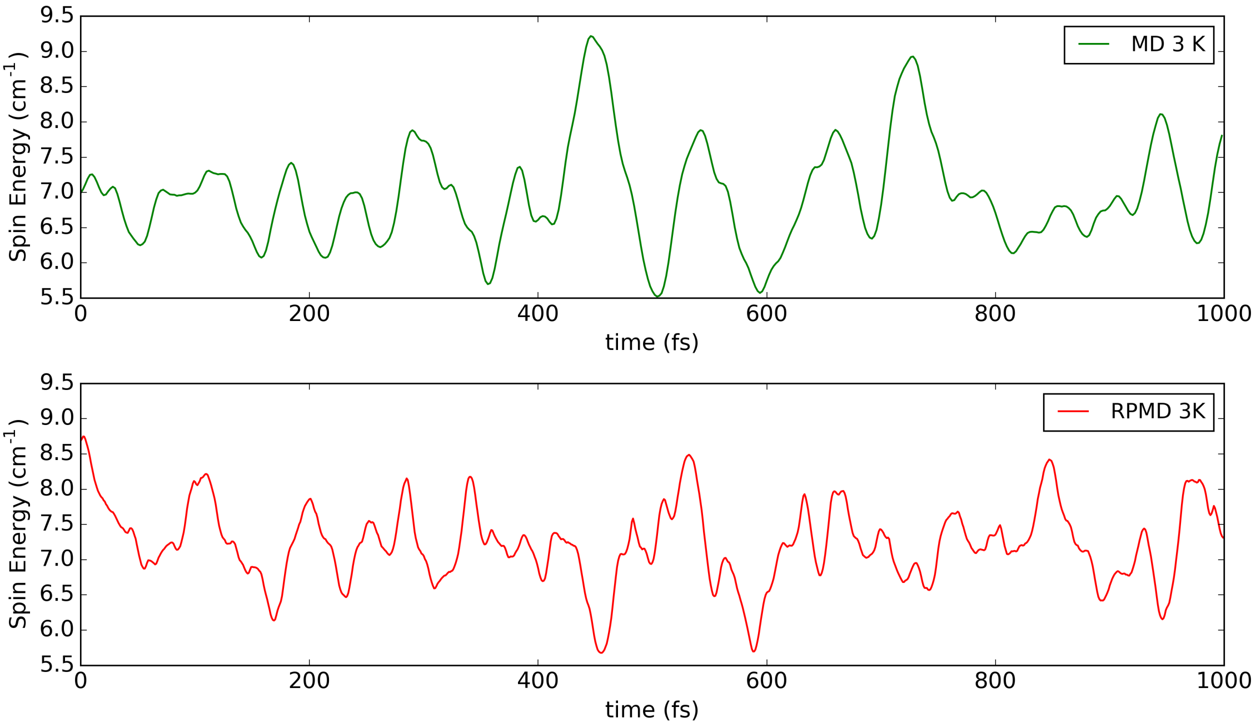

Figure S4.2.*Comparison between the spin energy fluctuations for the first excited state during two sample 1000 fs trajectories at 3 K, calculated by either AMBER MD, the technique employed in this work, or Ring Polymer Molecular Dynamics, which also introduces the effects of quantum tunneling.*

Figures S4.1 and S4.2 show the similarity between the results obtained as per the classical molecular dynamics methodology indicated in the present work *vs* the results including quantum nuclear effects through RPMD. As can be seen, there are no substantial differences after consideration of quantum effects, neither in the case of the distribution of energies of the different spin states (Fig. S4.1), nor for the qualitative evolution of the first excited state during a continuous picosecond (Fig. S4.2).

S5. Spin energy levels calculations using MD output as input

Once the MD calculations for the TbLBT system were done, it was possible to proceed with the ultimate goal, which was to estimate the influence of molecular motions of TbLBT in frozen solution on its electronic spin energy levels. The details of how the dynamics of molecular movements are coupled with the dynamics of electronic spins are subtle and not yet well understood. An effective coupling between them is only possible if the time scales of the protein motions and the spin dynamics of the system are similar. Diverse phenomena are involved in the dynamics of spin energy levels: among them optical excitations and magnetic relaxation. These phenomena occur at characteristic time scales and can range between ps for optical transitions, and fractions of ms for spin-lattice magnetic relaxation. To better comprehend the time scales of the molecular motion in our system, we aimed to estimate the spin energy levels within the ground J multiplet throughout the trajectory in the MD, employing the cartesian coordinates of the donor atoms involved in the lanthanide coordination.

Thus, the calculation of the spin energies for the 13 electron spin states of Tb^{3+} required, thus the extraction of the coordinates of the potential oxygens involved in the sphere coordination of the Tb^{3+} ion from the MD run. This was accomplished employing a fortran90 script (hack_atoms.F90) implemented in-house. This script requires an input file that defines the number of time steps between two consecutive extractions of coordinates, the number of atoms to extract the coordinates from, and the indexes of the relevant atoms whose coordinates are to be to be collected. The cartesian coordinates of atoms, from what we can think of as snapshots of the TbLBT molecule every a certain number of time steps, are written in the output file (HACK_ATOMS.txt) one line for time step. It has to be noted that the spacing between time steps was set in the MD simulations as 2 fs, and this has a consequence on how separated are the snapshots/frames we obtain. This script served to communicate with the parallel AMBER pmemd.cuda code (MPI). We obtained a txt file with the desired coordinates in a designated order.

The coordinates at each snapshot were therefore used as an input for SIMPRE 1.1,[13] a fortran77 code based on an effective electrostatic model of point charges around a lanthanide magnetic ion to estimate the spin energy levels based on the position (coordinates) of the atoms directly bound to the magnetic ion. This package allowed us to estimate the 13 electron spin energy levels of Tb^{3+} in a computationally efficient way. These 13 energy levels arise from the fact that the Tb^{3+} ion has a total angular momentum (J) of 6, and as such, the secondary total angular momentum (M_J) can take $2J + 1$ values. The package has already been successfully applied to several mononuclear systems with single-molecule magnetic behavior,[14] and, thanks to the parameterization of common ligands as effective charges, it is possible to build upon these results to not only rationalize but also predict the properties of more complex systems. In this context a well-tested geometrical model known as Radial Effective Charge (REC) model was used [15,16], which evaluates the crystal field effect by placing an effective charge along the lanthanide–ligand axes (Fig. S5). This effective charge,

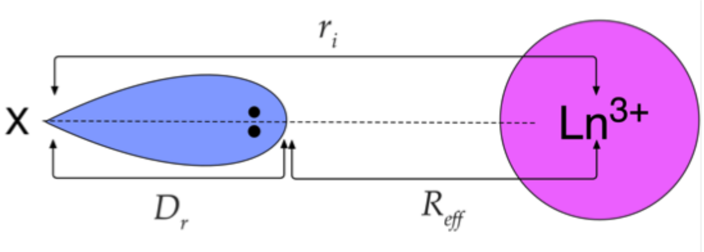

Figure S5. *Electronic pair of a ligand X oriented towards the nucleus of a trivalent lanthanide cation. The effective charge is located between the lanthanide and the donor atom at* $R_{eff} = R_i - D_r$*. Extracted with permission from the thesis of J. J. Baldoví, 2016.*[14]

which is smaller than the formal charge, and located at a closer distance compared with the crystallographic distance, reproduces the covalency effects.

As some of us did in a previous work,[4] we classify the donor atoms according to their formal charge, which can have values of 0.0, -0.5 and -1.0. Donor atoms of formal charge 0.0 correspond to non-charged oxygen atoms, as is the case of the oxygen belonging to the amide in Asn5, and the carbonyl oxygen in the Trp7 backbone. The formal charge of -1.0 is assigned when only one of the oxygen atoms belonging to a carboxylate group from an aspartate or glutamate aminoacid is coordinating the lanthanide, as can be the case of Asp3, Asp7, Glu11 and Glu14.

Table S5. *Criteria for radio reduction and effective charge assignation for the donor atoms, taking into account wether the metal-coordinating oxygens belong to the same aminoacid residue.*

Oxygen identifier	**Number of donor atoms belonging to same residue**	**D_r (Radius reduction)**	**Z_i (Effective charge)**
D3:OD1	0	0.895	0.105
D3:OD1	1	1.100	0.085
D3:OD2	0	0.895	0.105
D3:OD2	1	1.100	0.085
N5:OD1	-	1.350	0.069
D7:OD1	0	0.895	0.105
D7:OD1	1	1.100	0.085
D7:OD2	0	0.895	0.105
D7:OD2	1	1.100	0.085
W9:O	-	1.350	0.069
E11:OE1	0	0.895	0.105
E11:OE1	1	1.100	0.085
E11:OE2	0	0.895	0.105
E11:OE2	1	1.100	0.085
E14:OE1	0	0.895	0.105
E14:OE1	1	1.100	0.085
E14:OE2	0	0.895	0.105
E14:OE2	1	1.100	0.085
WAT:O	-	1.350	0.069

When both oxygen atoms belonging to the aminoacid residues above mentioned are coordinating the metal, then a formal charge -0.5 is assigned to each one of the two oxygens in the carboxylate group. A peculiarity of the present work is that the Molecular Dynamics simulations produce a series of snapshots of the atomic positions for all atoms involved in the lanthanide coordination (which we define taking the threshold of a maximum distance to the Tb^{3+} of 3 Å), so the coordinating oxygen atoms can be different in every time step. This allows to consider the possibility of atoms entering or exiting the coordination sphere. In practice, in a given timestep two oxygens belonging to the same carboxylate residue can be forming the coordination sphere, and in the next timestep only one of the two is.

The input files that SIMPRE1.1 requires are two. One defines the computational parameters and yes/no switches for the calculation (simpre.par). The second input file (simpre.dat) defines the coordinates for the oxygen atoms that act as ligands taking the metal atom (Tb^{3+} ion) as origin of coordinates, contains the effective point charge values for these atoms, and also defines some other output options.

This is the first application of REC and SIMPRE for dynamical fluctuations of the positions, but the robustness and applicability of SIMPRE in presence of small structural distortions is well stablished. A clear example is the work where the REC parameters proved to be robust against both (a) changing from one polyoxometalate to a completely different one that preserves approximately the coordination sphere and (b) a change in the lanthanide itself, which affects the coordination sphere because of the lanthanide contraction.[17] In this case, 10 different structures are described by 2 REC parameters, where 8 of the 10 are used to fit the parameters and the other 2 are used as an independent test. Moreover, in practice this meant the prediction of the single-ion magnet behavior of a Nd^{3+} complex (a metal that has rarely been reported as presenting these properties). Furthermore, there is indication that REC+SIMPRE are able, at least sometimes, to match *ab initio* calculations, when they are both tested against the real gold standard of spectroscopic information.[18]

S5.1. Python script to manage calculations of electronic spin energy levels for MD snapshots

The analysis of the MD results was performed using a python 2.7 script developed during the present work (see scheme in Fig. S5.1).

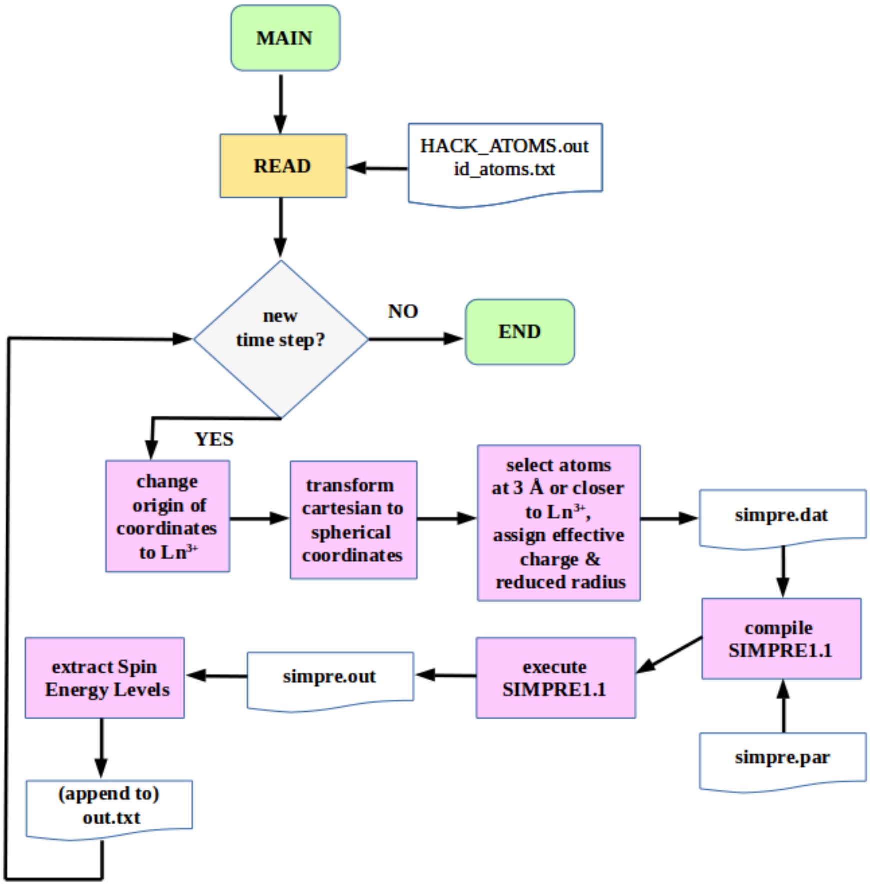

Figure S5.1. *Flowchart diagram showing the processing of each line from the input file HACK_ATOMS.out (each line containing coordinates for the* Tb^{3+} *ion and the other coordination atoms in a time step) in the amberHACK2simpre.py program.*

This python script uses as input a dat file containing the cartesian coordinates of Tb^{3+}-coordinated atoms, and a general simpre.par file, to estimate the spin energy levels for each MD snapshot. An additional input file (id_atoms.txt) was required to identify the procedence of the distinct oxygens that coordinate the metal, so that effective charges and reduced radius could be assigned before the generation of the simpre.dat file (see Table S5 and Fig. S5.1). The effective charges and reduced radius used are discussed in Rosaleny *et al.*, 2018.[4] The obtention of the spin energy levels using the script required the execution in a loop of SIMPRE1.1 for each snapshot.

S6. Spin Energy Levels at 3 K, 30 K and 300K

The spin energy levels for a series of time steps belonging to an isobaric isothermic MD simulation at 30 K were estimated using the approach explained in section S5. The coordinates of the atoms involved in the coordination sphere of Tb^{3+} (in the context of our system TbLBT) were obtained using the force field-based AMBER software in combination with a script developed in-house. These coordinates were used as input for our script (*amberHACK2simpre.py*), and the spin energy levels were calculated with SIMPRE1.1. The energy levels obtained were refered to the lowest one, so that the first level always had an energy value of 0 cm^{-1}.

The representation of the energies of the different spin states during the simulation can be seen in Fig. S6.1. The figure shows a large fluctuation of the spin energy for each particular level. For instance, for the second electronic spin energy level (plotted in aquamarine), the value of the energy in one time step experiences a big variation for the next time step (in this figure the time between data points plotted is 100 ps).

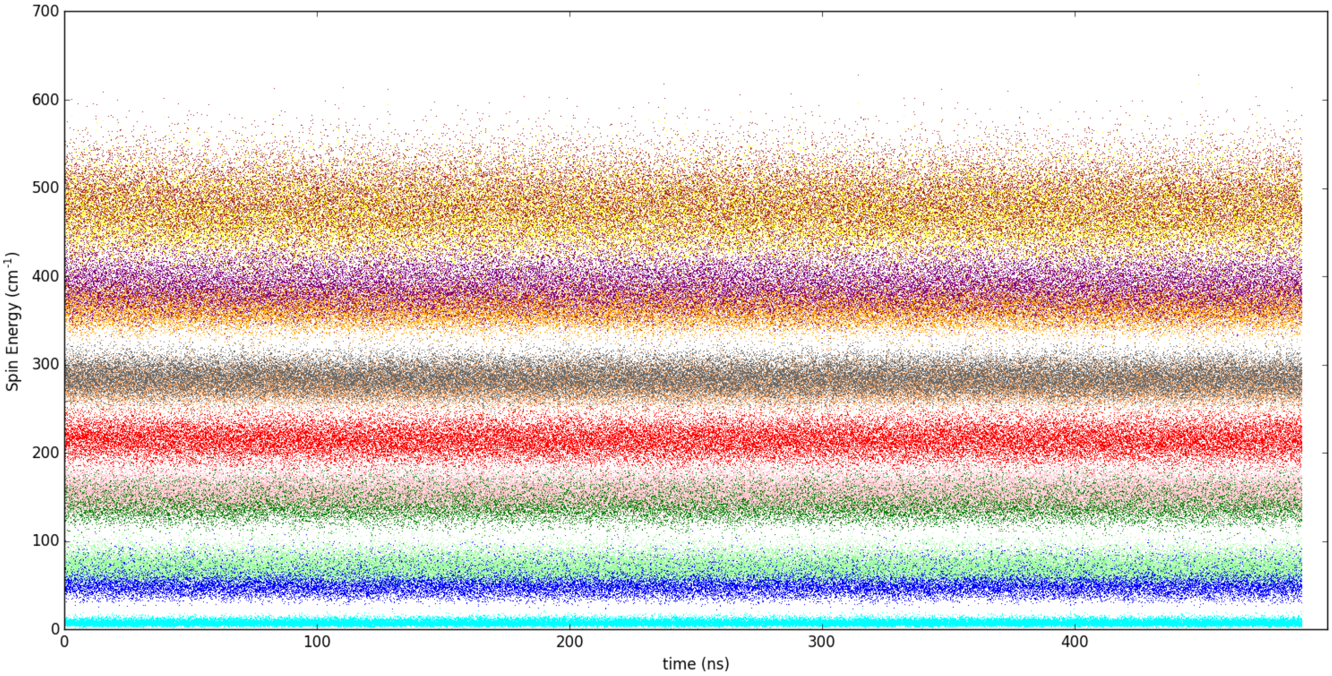

Figure S6.1. Spin energy levels in the ground *J* multiplet of TbLBT during a ~500 ns trajectory at 30 K as calculated by AMBER + SIMPRE, instantaneous energies.

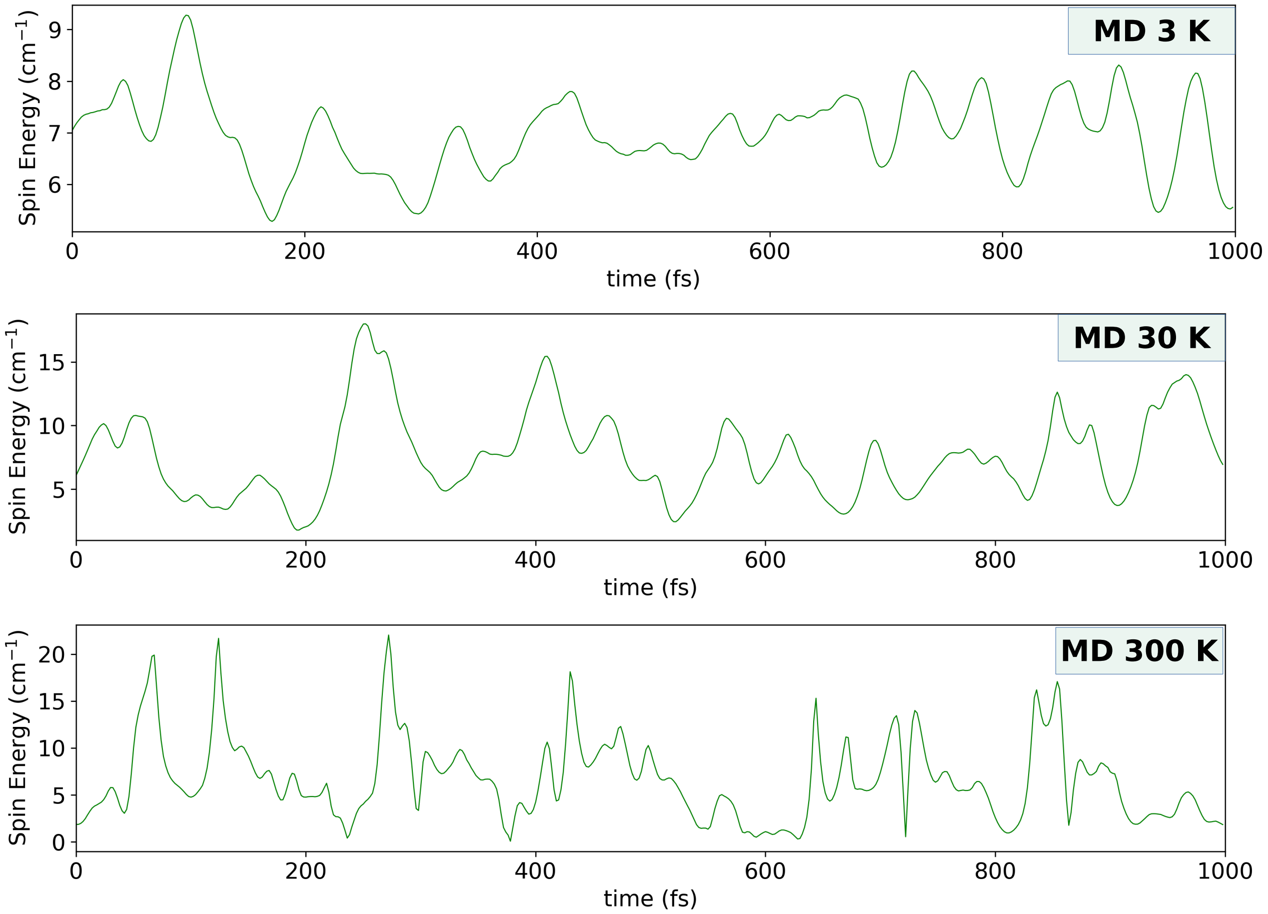

Figure S6.2. *Spin energy for the second level for MD at 3 K, 30 K and 300 K. All time steps produced for the depicted MD run are plotted for 1 ps.*

S7. Autocorrelation plots

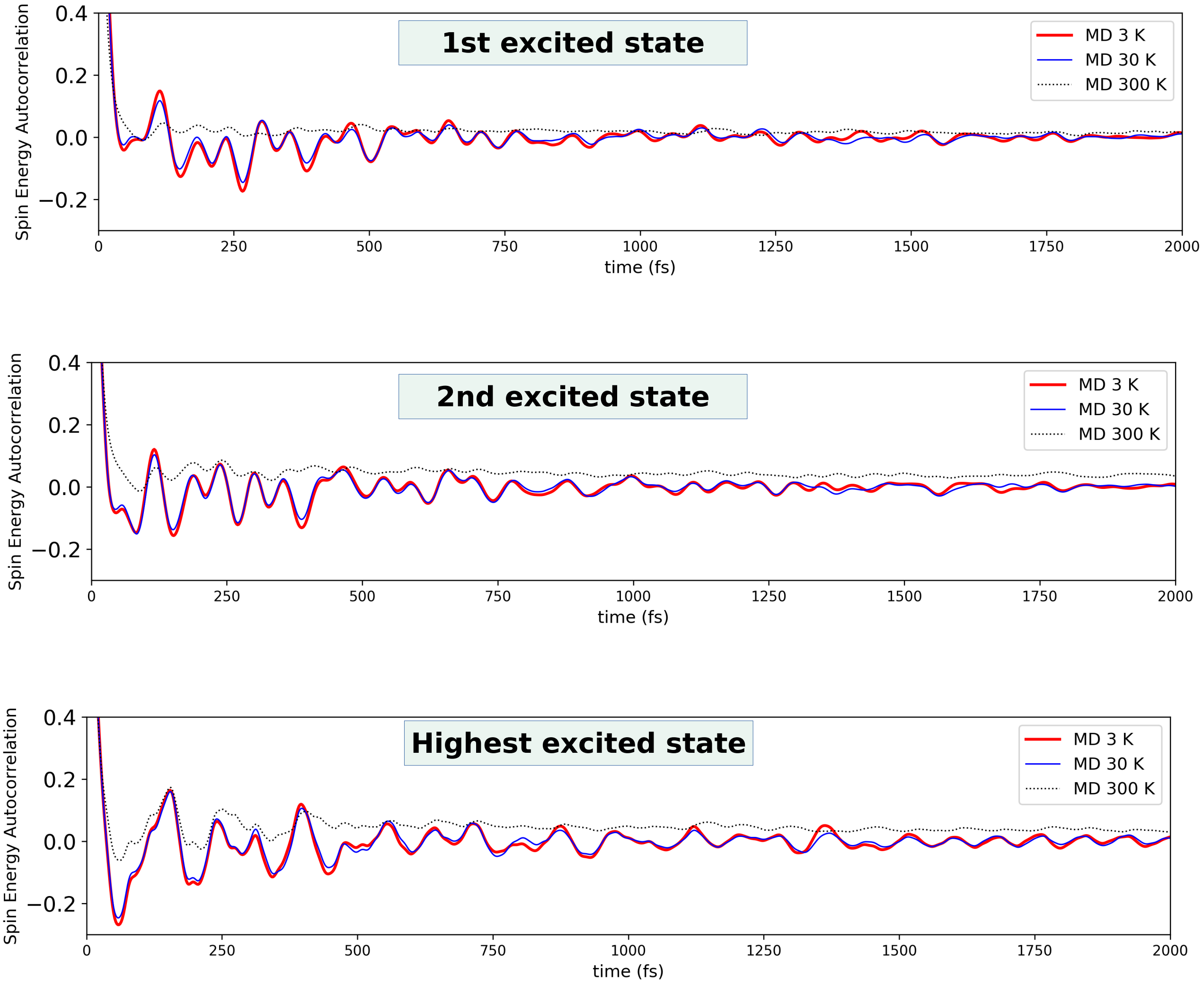

Figure S7. *Autocorrelation plots of the spin energy levels for the first, second and highest excited spin states of the ground J multiplet resulting from the MD simulations at 3 K, 30 K, and 300K.*

S8. References

(1) Nitz, M.; Sherawat, M.; Franz, K. J.; Peisach, E.; Allen, K. N.; Imperiali, B. Structural Origin of the High Affinity of a Chemically Evolved Lanthanide-Binding Peptide. *Angew. Chem. Int. Ed Engl.* **2004**, *43* (28), 3682–3685. https://doi.org/10.1002/anie.200460028.

(2) Qiao, B.; Skanthakumar, S.; Soderholm, L. Comparative CHARMM and AMOEBA Simulations of Lanthanide Hydration Energetics and Experimental Aqueous-Solution Structures. *J. Chem. Theory Comput.* **2018**, *14* (3), 1781–1790. https://doi.org/10.1021/acs.jctc.7b01018.

(3) Martínez, L.; Andrade, R.; Birgin, E. G.; Martínez, J. M. PACKMOL: A package for building initial configurations for molecular dynamics simulations. *J. Comput. Chem.* **2009**, *30* (13), 2157–2164. https://doi.org/10.1002/jcc.21224.

(4) Rosaleny, L. E.; Cardona-Serra, S.; Escalera-Moreno, L.; Baldoví, J. J.; Gołębiewska, V.; Wlazło, K.; Casino, P.; Prima-García, H.; Gaita-Ariño, A.; Coronado, E. Peptides as Versatile Platforms for Quantum Computing. *J. Phys. Chem. Lett.* **2018**, *9* (16),4522–4526. https://doi.org/10.1021/acs.jpclett.8b01813.

(5) Salomon-Ferrer, R.; Case, D. A.; Walker, R. C. An Overview of the Amber Biomolecular Simulation Package. *Wiley Interdiscip. Rev. Comput. Mol. Sci.* **2013**, *3* (2), 198–210. https://doi.org/10.1002/wcms.1121.

(6) Maier, J. A.; Martinez, C.; Kasavajhala, K.; Wickstrom, L.; Hauser, K. E.; Simmerling, C. Ff14SB: Improving the Accuracy of Protein Side Chain and Backbone Parameters from Ff99SB. *J. Chem. Theory Comput.* **2015**, *11* (8), 3696–3713. https://doi.org/10.1021/acs.jctc.5b00255.

(7) Jorgensen, W. L.; Chandrasekhar, J.; Madura, J. D.; Impey, R. W.; Klein, M. L. Comparison of Simple Potential Functions for Simulating Liquid Water. *J. Chem. Phys.* **1983**, *79* (2), 926–935. https://doi.org/10.1063/1.445869.

(8) Wang, J.; Wolf, R. M.; Caldwell, J. W.; Kollman, P. A.; Case, D. A. Development and Testing of a General Amber Force Field. *J. Comput. Chem.* **2004**, *25* (9), 1157–1174. https://doi.org/10.1002/jcc.20035.

(9) Ryckaert, J.-P.; Ciccotti, G.; Berendsen, H. J. C. Numerical Integration of the Cartesian Equations of Motion of a System with Constraints: Molecular Dynamics of n-Alkanes. *J. Comput. Phys.* **1977**, *23* (3), 327–341. https://doi.org/10.1016/0021-9991(77)90098-5.

(10) Habershon, S.; Manolopoulos, D. E.; Markland, T. E.; Miller, T. F. Ring-Polymer Molecular Dynamics: Quantum Effects in Chemical Dynamics from Classical Trajectories in an Extended Phase Space. *Annu. Rev. Phys. Chem.* **2013**, *64* (1), 387–413. https://doi.org/10.1146/annurev-physchem-040412-110122.

(11) Kapil, V.; Rossi, M.; Marsalek, O.; Petraglia, R.; Litman, Y.; Spura, T.; Cheng, B.; Cuzzocrea, A.; Meißner, R. H.; Wilkins, D. M.; et al. I-PI 2.0: A Universal Force Engine for Advanced Molecular Simulations. *Comput. Phys. Commun.* **2019**, *236*, 214–223. https://doi.org/10.1016/j.cpc.2018.09.020.

(12) Ceriotti, M.; Parrinello, M.; Markland, T. E.; Manolopoulos, D. E. Efficient Stochastic Thermostatting of Path Integral Molecular Dynamics. *J. Chem. Phys.* **2010**, *133* (12), 124104. https://doi.org/10.1063/1.3489925.

(13) Baldoví, J. J.; Cardona-Serra, S.; Clemente-Juan, J. M.; Coronado, E.; Gaita-Ariño, A.; Palii, A. SIMPRE: A Software Package to Calculate Crystal Field Parameters, Energy Levels, and Magnetic Properties on Mononuclear Lanthanoid Complexes Based on Charge Distributions. *J. Comput. Chem.* **2013**, *34* (22), 1961–1967.

(14) Baldoví, J. J. Rational design and modelling of f-block molecular nanomagnets. Doctoral Dissertation, Universitat de València, 2016. http://ir.uv.es/6YTdtjj

(15) Baldoví, J. J.; Borrás-Almenar, J. J.; Clemente-Juan, J. M.; Coronado, E.; Gaita-Ariño, A. Modeling the Properties of Lanthanoid Single-Ion Magnets Using an Effective Point-Charge Approach. *Dalton Trans.* **2012**, *41* (44), 13705–13710. https://doi.org/10.1039/c2dt31411h.

(16) J. Baldoví, J.; Gaita-Ariño, A.; Coronado, E. Modeling the Magnetic Properties of Lanthanide Complexes: Relationship of the REC Parameters with Pauling Electronegativity and Coordination Number. *Dalton Trans.* **2015**, *44* (28), 12535–12538. https://doi.org/10.1039/C5DT01839K.

(17) Baldoví, J. J.; Clemente-Juan, J. M.; Coronado, E.; Duan, Y.; Gaita-Ariño, A.; Giménez-Saiz, C. Construction of a General Library for the Rational Design of Nanomagnets and Spin Qubits Based on Mononuclear F-Block Complexes. The Polyoxometalate Case. *Inorg. Chem.* **2014**, *53* (18), 9976–9980. https://doi.org/10.1021/ic501867d.

(18) Baldoví, J. J.; Duan, Y.; Morales, R.; Gaita-Ariño, A.; Ruiz, E.; Coronado, E. Rational Design of Lanthanoid Single-Ion Magnets: Predictive Power of the Theoretical Models. *Chem. – Eur. J.* **2016**, *22* (38), 13532–13539. https://doi.org/10.1002/chem.201601741.